

The High-Pressure Chemistry of Iron*

H. G. DRICKAMER, V. C. BASTRON, D. C. FISHER, AND D. C. GRENOBLE

*Department of Chemistry and Chemical Engineering and Materials Research Laboratory,
University of Illinois, Urbana, Illinois 61801*

Received December 4, 1969

The high-pressure chemistry of iron in the solid state is rich in new phenomena. Optical studies of the effect of pressure on the interelectronic repulsion parameters and the ligand-to-metal charge transfer peaks, as well as Mössbauer resonance measurements of the change of isomer shift with pressure, indicate that with increasing pressure the $3d$ orbitals lower in energy vis-à-vis the ligand orbitals. This has important effects on both the oxidation state and spin state of iron.

With increasing pressure Fe(III) reduces to Fe(II) in a wide variety of compounds. This process is analyzed in considerable detail. Examples of the reduction of Fe(IV) to Fe(III) and of Fe(VI) to Fe(IV) and Fe(III) are discussed briefly. The ferrocyanides are the classical low-spin iron compounds. The strong bonding is in part due to the back donation of iron $t_{2g}(\pi)$ electrons to the empty π^* orbitals of the cyanide. The increased affinity of iron for electrons at high pressure reduces this back donation and results in a partial conversion to high-spin Fe(II). The effect of pressure on the spin state of ferricyanides reduced at high pressure, and on substituted cyanides, especially nitroprussides, is also considered. Two cases of special interest, Prussian blue, $\text{Fe}_4[\text{Fe}(\text{CN})_6]_3$, and ferrous nitroprusside, $\text{Fe}[\text{Fe}(\text{CN})_5\text{NO}]$, are discussed at some length.

Introduction

Studies of the effect of pressure on electronic behavior in compounds of iron have revealed a number of new phenomena that have significance for many branches of science.

The tools used in these investigations have been primarily Mössbauer resonance, and, in lesser degree, optical absorption. It is useful to review briefly what can be observed with these tools and what is known about the effects of pressure on the electronic behavior of transition metal complexes.

Emission of a gamma ray occurs when a radioactive nucleus decays from an excited state to a lower level. The nuclear energy levels are measurably sensitive to electronic wave functions having non-zero amplitude at the nucleus (s wave functions). Thus, ^{57}Fe in a stainless steel source is not in resonance with ^{57}Fe in, say, a ferric chloride absorber. By moving the source with respect to the absorber, one can establish resonance, making use of the Doppler velocity. A Mössbauer spectrometer is a device for producing and measuring accurately the velocities necessary to establish resonance between

a source and absorber with different chemical environments. These energy differences are given in mm/sec; for ^{57}Fe , 1 mm/sec corresponds to a difference in energy of the order of 10^{-4} cal/mole.

The primary readout from Mössbauer resonance is the center of gravity of the spectrum, known as the isomer shift. In this work, we are interested in changes in isomer shift with changes in the environment. The $1s$ and $2s$ orbitals are strongly isolated from the environment. The $3s$ electrons do not interact directly with the ligands either, but the radial maximum of their orbitals is at about the same point as that of the $3d$ orbitals which, of course, interact strongly with the ligand orbitals. From changes in the isomer shift we can infer information concerning changes in the occupation and radial extent of the $3d$ orbitals, and thus about changes in the oxidation state and chemical bonding of iron.

The second readout of interest here is the quadrupole splitting—the interaction between the nuclear quadrupole moment and an electric field gradient at the nucleus. This interaction partially removes the degeneracy of the excited state of spin $3/2$, and gives two peaks in the spectrum instead of one. The possible sources of an electric field gradient include a noncubic arrangement of the ligands and an

* This research was supported in part by the U.S. Atomic Energy Commission under Contract AT(11-1)-1198.

aspherical occupation of the partially filled $3d$ shell. The latter cause, when present, is dominant because of the relatively short range of the quadrupolar forces. In a free ion, and normally in an ionic compound, the $3d$ orbitals are filled to give maximum multiplicity, according to Hund's rule. A high-spin ferric ion with five $3d$ electrons, one in each of five available levels, presents a spherically symmetric field, so any quadrupole splitting depends strictly on the noncubic arrangement of the ligands. Since the extra $3d$ electron of the ferrous ion is never *smearred out* in a spherically symmetric manner over the $3d$ orbitals, high spin ferrous systems exhibit large quadrupole splittings. If the interaction between ligand and metal is sufficiently strong, it may be energetically advantageous to pair the electron spins. A low-spin ferrous ion exhibits little or no quadrupole splitting, while a low-spin ferric ion exhibits significantly more.

Typical values for isomer shifts and quadrupole splittings are presented in Table I. The high-spin ferrous ion [Fe(II)] has a relatively large isomer shift, which corresponds to a relatively low electron density at the nucleus. This is consistent with the fact that there are six $3d$ electrons shielding the $3s$ electrons. As discussed above, there is a large quadrupole splitting. The ferric ion [Fe(III)] exhibits a significantly smaller isomer shift (larger electron density at the nucleus). In large part this is due to the decreased shielding of the $3s$ electrons, since there are nominally only five $3d$ electrons. The quadrupole splitting is usually modest unless the external symmetry is very far from cubic. There exist higher oxidation states of iron—Fe(IV), nominally a $3d^4$ ion, and Fe(VI), nominally a $3d^2$ ion. These exhibit increased electron density at the nucleus as is expected from the reduced shielding of the $3s$ orbitals. Their quadrupole splitting has not been analyzed in any detail.

TABLE I
TYPICAL ISOMER SHIFT AND QUADRUPOLE SPLITTING
(mm/sec)

	Isomer Shift (Rel. to Iron Metal)	Quadrupole Splitting
Fe(II) high spin	1.3–1.4	2.0–3.0
Fe(III) high spin	0.3–0.5	0.3–0.5
Fe(IV) (ferrate)	(–0.1)–(0.0)	—
Fe(VI) (ferrate)	(–0.9)–(–0.8)	—
Ferrocyanide	(–0.1)–(0.0)	~ 0
Ferricyanide	(–0.1)–(0.0)	0.3–0.6
Nitroprusside	(–0.3)–(–0.2)	1.6 2.0

By far, the most widely studied of the low-spin compounds of iron are the ferrocyanides, ferricyanides, and substituted cyanides. Although these nominally contain six $3d$ electrons (five for the ferricyanides) they exhibit a relatively small isomer shift (high electron density at the nucleus), because the $3d$ electrons are very strongly delocalized, due to covalent interaction with the ligand orbitals. This fact will be of great importance in the latter part of the paper. The quadrupole splittings can be accounted for on the basis of our earlier discussion—the large value for the nitroprusside ion is caused by the strongly distorted ligand field.

A $3d$ electron on a free ion of iron can exist in a series of fivefold degenerate energy levels. The difference in energy between the ground state and the excited states is due to the difference in interelectronic repulsion in the various configurations. Their energy differences can most conveniently be expressed in terms of the Racah parameters A , B , and C . In a field of less than spherical symmetry, the degeneracy is partially removed. For octahedral symmetry, one obtains a threefold degenerate (t_{2g}) set of levels with orbitals concentrated between the ligands (π symmetry) and a doubly degenerate set of (e_g) levels of higher energy, having σ symmetry. The splitting between these levels is a measure of the ligand field called $10 Dq$ or Δ . For other symmetries, the splittings vary but none of the phenomena discussed here would be qualitatively different. Optical transitions of relatively low-intensity measure Δ or combinations of Δ and the Racah parameters B and C in the complex. For a ferrous ion in a typical ionic crystal, Δ values are on the order of $8000\text{--}9000\text{ cm}^{-1}$ ($1\text{--}1.1\text{ eV}$), while $B \cong C/4$ is of the order of 900 cm^{-1} . If the ligand field reaches a value of $14,000\text{--}16,000\text{ cm}^{-1}$, one may obtain a spin paired state, as mentioned above. The ferrocyanides and related compounds exhibit a ligand field $\Delta \sim 32,000\text{--}36,000\text{ cm}^{-1}$ and a value of the Racah parameter $B \sim 400\text{ cm}^{-1}$. The low value of the interelectronic repulsion parameter indicates the strong delocalization of the $3d$ orbitals and is consistent with the low value of the isomer shift mentioned above.

There exists, in most transition metal ion complexes, a very intense transition with a peak center at $24,000\text{--}40,000\text{ cm}^{-1}$ ($3\text{--}5\text{ eV}$), and with a long tail which extends into and even through the visible region of the spectrum. This represents a charge transfer from the ligand nonbonding levels to the $3d$ orbitals of the metal ion.

With pressure, a number of changes are observed which make a consistent picture (1, 2). For high-

spin complexes, the ligand field parameter, Δ , increases by 12–15% in 150 kbar, while the Racah parameters decrease by 10–12% in the same range. The isomer shifts for these complexes decrease by 0.1–0.12 mm/sec in this range of pressure, i.e., the electron density at the iron nucleus increases by 10–15% of the difference between ordinary ferrous and ferric compounds—not an insignificant change. The charge transfer peaks shift to lower energy with increasing pressure, sometimes by as much as several thousand wave numbers in 150 kbar. If one presumes that the radial maximum of the 3d orbitals spreads with increasing pressure due to interaction with the ligands, this accounts for the decrease in B and C , since the interelectronic repulsion decreases as the electron-electron distance increases. It also explains the increased electron density at the iron nucleus, as the 3s orbitals are less shielded, and the red shift of the charge transfer peak, since the spreading of the 3d orbitals decreases their energy vis-à-vis the ligand nonbonding orbitals. More accurately, the 3d orbitals increase in energy with pressure less rapidly than do the ligand orbitals.

The Oxidation State of Iron

It has been observed in this laboratory (2–8) that ferric ion reduces to ferrous ion with increasing pressure, and that this is a reversible process, with some hysteresis. The phenomenon can be understood qualitatively in terms of the observations discussed above, plus a schematic configuration coordinate diagram (Fig. 1). Here, the ordinate is potential energy, and the abscissa is typically some vibrational mode of the system which aids electron transfer. Optical transitions are rapid compared with lattice vibrations and thus occur vertically on such a diagram, in accordance with the Franck–Condon principle. Thermal transitions are not subject to this limitation. The reduction is accomplished by transfer of an electron from a nonbonding ligand orbital to

O = OPTICAL TRANSITION
T = THERMAL TRANSITION

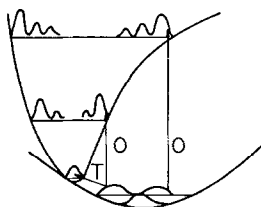


FIG. 1. Schematic configuration coordinate diagram.

the metal 3d antibonding orbital—the charge transfer process discussed above. The steep slope of the excited state potential well is consistent with the long tail observed on the optical charge transfer peak. It can be seen that the thermal transfer may involve relatively small energy, so that the observed red shift of the optical peaks is sufficient to establish a new ground state.

One would expect from the above description that complete reduction would occur over a relatively narrow pressure range—such that the excited state potential well lowers in energy by about kT with respect to the ground state. In fact, the reduction takes place continuously over a wide pressure range. For most systems the relationship between concentration and pressure can be expressed in the form,

$$K = \frac{C_{II}}{C_{III}} = AP^B, \quad (1)$$

where C_{II} and C_{III} are the concentrations (actually the *site fractions*) of ferrous and ferric sites, and A and B are constants, so that $\ln K$ is a linear function of $\ln P$. Consecutive runs at the same pressure gave the same conversions, so that the observations involved an equilibrium phenomenon, not the result of slow kinetics. The constants A and B for a variety of systems appear in Table II. Figures 2–4 show typical data. In Fig. 2 are shown FeCl_3 , FeBr_3 , and $\text{Fe}(\text{NCS})_3$. These systems have in common the fact that ligands are shared between adjacent iron ions so that there is strong coupling between sites. The slope of the line is ~ 0.5 —a relatively small value, as we shall see. Figure 3 exhibits data for two hydrates and ferric acetylacetonate. For these cases there is little or no sharing of ligands between sites, and the slope is ~ 1.0 . In

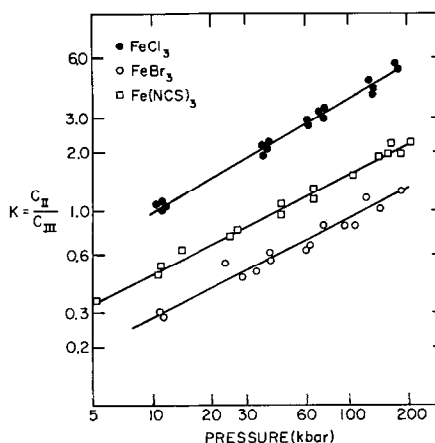


FIG. 2. $\ln K$ vs $\ln P$ —crystals with strong coupling between sites.

TABLE II
CONSTANTS A AND B FOR THE RELATIONSHIP $K = AP^B$

Material	Temperature °K	A	B
FeCl ₃	295	0.265	0.564
FeBr ₃	295	0.076	0.426
KFeCl ₄	295	0.091	0.497
FePO ₄	295	0.079	0.457
Fe citrate	295	0.112	0.350
K ₃ Fe(CN) ₆	295	0.109	2.06
Fe acetylacetonate	295	1.2×10^{-5}	2.23
Fe acetylacetonate	375	0.96×10^{-2}	1.01
Fe basic acetate	378	0.22×10^{-6}	3.05
Fe basic acetate	418	2.21×10^{-2}	0.98
Fe oxalate	295	0.041	0.51
Fe oxalate	335	0.029	0.83
Fe oxalate	383	0.043	1.146
Strontium Fe oxalate	295	0.115	0.301
Strontium Fe oxalate	383	0.058	0.844
FeCl ₃ · 6H ₂ O	294	0.063	0.95
FeF ₃ · 3H ₂ O	294	0.027	0.95
FeF ₃ · 3H ₂ O plus excess H ₂ O	294	0.072	0.95
FeCl ₃ · 6NH ₃ < 25 kbar	294	2.4×10^{-6}	4.06
FeCl ₃ · 6NH ₃ > 25 kbar	294	0.46	0.27
Fe(NCS) ₃ · 6H ₂ O	295	0.136	0.528
K ₃ Fe(NCS) ₆	295	0.024	0.692
Hemin	294	5.5×10^{-3}	1.53
Hemin	335	4.2×10^{-4}	2.04
Hemin	367	3.5×10^{-5}	2.57
Hematin	294	2.7×10^{-5}	2.67
Hematin	343	1.4×10^{-7}	3.77

Fig. 4 are shown conversion data for hemin and hematin. These are prototype molecules for hemoglobin, and thus are of biological interest. They form molecular crystals with very little coupling

between sites. The slope B is in the range 2.5–3.0. From these results one can get a qualitative understanding of the pressure dependence of the conversion. When an Fe(III) ion on a given site is reduced,

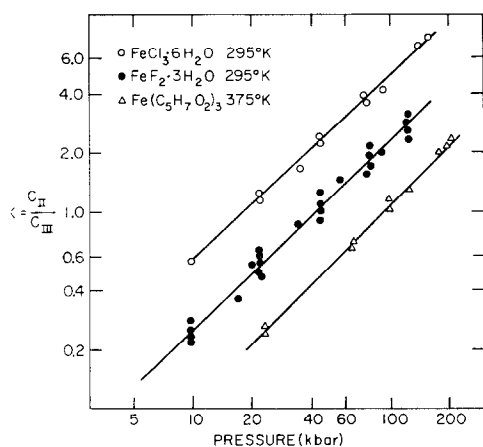


FIG. 3. $\ln K$ vs $\ln P$ —Crystals with moderate coupling between sites.

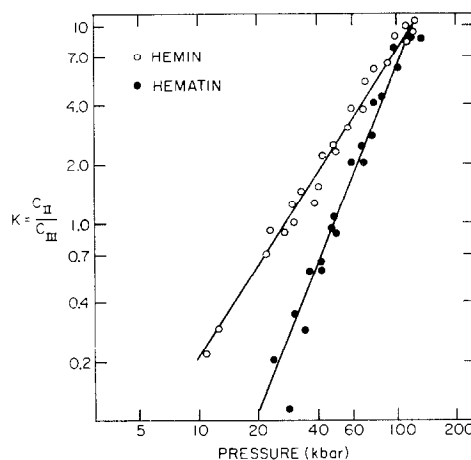


FIG. 4. $\ln K$ vs $\ln P$ —Crystals with weak coupling between sites.

an electrical polarization, and possibly a mechanical strain is introduced. This perturbs the potential wells at neighboring sites and makes the conversion of these sites more difficult. The greater the coupling between sites, the stronger this interaction and the lower the slope of the $\ln K$ vs $\ln P$ curve. Those systems with the most coupling between sites show the most hysteresis on release of pressure. In all cases, when the sample is powdered, it returns completely to the ferric state.

A simple thermodynamic analysis may be helpful in visualizing the interaction between sites in macroscopic terms. The equilibrium constant defined above can be written

$$K = e^{-\Delta\bar{G}/RT}; \quad (2)$$

then

$$\frac{\partial \ln K}{\partial \ln P} = B = -\frac{P\Delta\bar{V}}{RT}, \quad (3)$$

where $\Delta\bar{V}$ is the difference in partial molar volume of products and reactants. A rearrangement of (3) gives

$$\frac{\partial \ln C_{II}}{\partial \ln P} = \frac{P(\bar{V}_{III} - \bar{V}_{II})}{RT} C_{III}. \quad (4)$$

Thus, the fractional increase in sites converted for a given fractional increase in pressure is proportional to the fraction of unconverted sites. The coefficient of proportionality is the work to convert a site, measured in thermal units, i.e., units of RT . Over the range of concentration observable (8–92%) and in the pressure ranges 5–200 kbar, within our accuracy, this work is independent of concentration or pressure. It should be pointed out that not all systems gave the strictly linear relationship between $\ln K$ and $\ln P$. Further, the concentrations used in this work were obtained by computer fitting Lorentzian curves to the data. In addition to the errors inherent in this process, there is a definite possibility that the f number at a converted site is different, or has a different pressure dependence, than that for a ferric site. Nevertheless, it is clear that for the vast majority of systems $\Delta\bar{V}$ must be a strong function of pressure, or of concentration. One can express this in two different ways. As indicated earlier, when a site converts, a free radical is formed at a ligand site, or a hole circulates among the adjacent ligands. There results a mechanical strain and a corresponding stress. One can insert into $d\bar{G}$ terms of the form $-\sum_i \epsilon_i d\sigma_i$, where ϵ_i and σ_i are the strains and stresses. Then

$$\Delta\bar{V} = \Delta V_0 - \sum_i \epsilon_i \frac{\partial \sigma_i}{\partial P}, \quad (5)$$

where ΔV_0 is the difference in volume of *pure* ferric and converted material—presumably a small number, and in any case, a constant. Alternatively, one can employ the language of solution theory. Using the standard analysis,

$$\Delta\bar{V} = \Delta V_0 - \frac{\partial V_e}{\partial C_{II}}, \quad (6)$$

where V_e is the excess volume of mixing. If one inserts typical data into (6), one finds that V_e is strongly dependent on concentration (or pressure), especially at low conversions, for those systems with strong coupling between sites. For systems like hemin and hematin with very weak coupling between sites, V_e varies little with concentration. In the limit of zero coupling, V_e would be identically zero for all concentrations and pressures, and the transformation would be complete in an extremely narrow range of pressure.

Heats of reaction have been obtained both by comparing points along different isotherms and from data taken along isobars. Typical values are given in Table III. For almost all systems studied, the reaction is endothermic, i.e., the yield increases

TABLE III
HEATS OF REACTION

Material	Pressure (kbar)	Temperature °K	H (eV)
FeCl ₃	*	323	0.12
FeCl ₃	*	393	0.18
FeBr ₃	*	323	0.20
FeBr ₃	*	393	0.32
KFeCl ₄	*	323–393	0.07
Fe acetylacetonate	60	325	0.15
Fe acetylacetonate	60	375	0.25
Fe acetylacetonate	150	325	0.065
Fe acetylacetonate	150	375	0.085
Fe basic acetate	75	398	0.93
Fe basic acetate	150	398	0.44
Fe oxalate	25	315	0.19
Fe oxalate	25	360	0.34
Fe oxalate	100	315	0.26
Fe oxalate	100	360	0.42
Strontium Fe oxalate	20	333	0.11
Strontium Fe oxalate	200	333	0.24
Hemin	20	335	–0.22
Hemin	60	335	–0.11
Hemin	90	335	–0.057
Hematin	40	320	–0.23
Hematin	90	320	–0.052

* Independent of pressure.

with increasing temperature. This is very reasonable as it takes thermal energy to cross the barrier between the potential wells. Hemin and hematin exhibited exothermic behavior. It would seem that thermal deformation of the potential wells must be the dominating effect for these systems.

High pressure studies have also been made on higher oxidation states of iron (9). SrFeO₃ contains Fe(IV). With pressure, this reduces to Fe(III). At 150 kbar, one observes about 65% Fe(III). The linear relationship between $\ln K$ and $\ln P$ is not obeyed. In BaFeO₄ iron is in the form Fe(VI). This apparently reduces to Fe(IV), with some production of Fe(III). The Fe(VI) is about 90% reduced at 150 kbar although impurities in the sample complicate the interpretation. It is evident that the ligand to metal electron transfer process is a very general one.

The Spin State of Iron

As was discussed in the Introduction, in a normal ionic compound or complex the 3d electrons on iron assume a configuration of maximum multiplicity. For the ferrous ion, when the ligand field parameter Δ approaches a value somewhat less than 2 eV, the balance between kinetic and potential energy begins to favor the low-spin arrangement. Since the crystal field tends to increase with pressure, one might expect that systems with a ligand field not too far below the critical value would undergo a high- to low-spin transition with increasing pressure. This transition, indeed, has been observed (10), but it is not the main point of the present discussion.

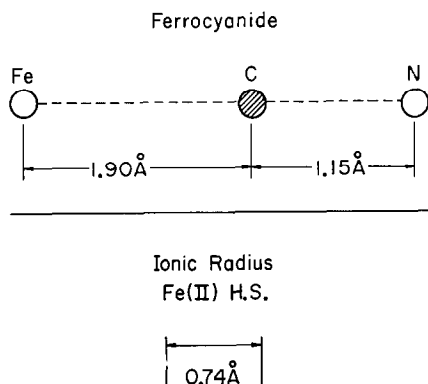
The ferrocyanides, ferricyanides, and substituted cyanides constitute perhaps the most interesting, and certainly the most widely studied, group of low-spin iron compounds. In these materials, the iron is surrounded in basically octahedral symmetry by six cyanide ions. (In the substituted cyanides, one of the CN⁻ is replaced by a different group and there may be a strong distortion from octahedral symmetry.) The iron is coordinated to the carbon end of the cyanide ion. The high-electron density at the iron nucleus (low isomer shift) and the small value for the interelectronic repulsion parameter both indicate that the 3d orbitals are strongly delocalized. The delocalization can be understood as follows. The cyanide ions have empty π^* orbitals. These can bond to the (filled) $t_{2g}(\pi)$ orbitals of the metal atom by *back donation* of metal electrons to the cyanide orbitals. Clearly, the degree of this back donation depends on the difference in energy between the π^* and t_{2g} orbitals. It is large when this energy difference is small and decreases as the energy

difference increases. This is an important point for our later discussion.

In this laboratory, we have observed the Mössbauer spectrum of five ferrocyanides—K₄Fe(CN)₆, Na₄Fe(CN)₆, Zn₂Fe(CN)₆, Ni₂Fe(CN)₆, and Cu₂Fe(CN)₆ (11)—to pressures of 200 kbar and temperatures of 150°C. At high pressure and high temperature an unexpected phenomenon occurred. A pair of peaks appeared in the spectrum with an isomer shift in the range 1.0–1.2 mm/sec and a quadrupole splitting ~ 2.0 mm/sec. These increased in intensity as either the pressure or temperature was increased. The possible explanations seem to be that one is producing either low-spin Fe(I) or high-spin Fe(II). It is known that the CN⁻ ligand has some tendency to stabilize low oxidation states, and the observed isomer shifts and quadrupole splitting are in a possible range for low-spin Fe(I). However, it is difficult to see how there would be energy available to transfer an electron to the e_g levels, some 4 eV above the filled t_{2g} levels. While this explanation cannot be completely discounted, there is a strong body of evidence that points towards the formation of high-spin Fe(II). The isomer shifts and quadrupole splitting lie within, but at the lower edge, of the usual range for high spin Fe(II). The conversion was reversible, but with considerable hysteresis. We were able to quench a sample of the copper salt which retained 18% conversion at one atmosphere according to its Mössbauer spectrum. A very sensitive Faraday balance indicated that this material had a magnetic susceptibility 1.75 times that of the starting material. This would indicate a conversion to high spin of 15–21% depending on whether one uses a *spin only* basis or ratios between susceptibilities of known low- and high-spin ferrous compounds. The infrared spectrum also revealed consistent information. In ordinary ferrocyanide the C \equiv N stretching frequency is at 2180 cm⁻¹, a relatively low value compared with that for the free cyanide ion. The Fe–C stretching frequency is at 494 cm⁻¹. On the quenched sample there was a definite shoulder at 2260 cm⁻¹, much nearer the free cyanide value, and a peak at 467 cm⁻¹. Both of these observations are consistent with reduced metal to carbon bonding, which one would expect for high-spin Fe(II). (See also the discussion of Fe[Fe(CN)₅NO] below.) A weak peak appeared at 11,800 cm⁻¹. This could be the crystal field peak of high-spin Fe(II). The uv spectrum was very poor, but it seemed that the transitions measuring the low-spin crystal field were shifted to lower energy.

A low- to high-spin transition with increasing pressure seems at first paradoxical in that for free

ions the low-spin ion would have the smaller volume. However, one must keep in mind that it is the volume of the system as a whole that must be considered. In ferrocyanides the bond distances are as shown below.



If one can speak of the *radius* of carbon in these circumstances, it must surely be less than 1.15 Å. The radius of high-spin Fe(II) is 0.74 Å. Thus, we can see that the delocalization of the iron orbitals results in a relatively large Fe–C distance, and a more compact high-spin arrangement is conceivable.

Let us first characterize the transition and then discuss the possible cause. Figure 5 shows the fraction of high spin versus pressure. The copper salt shows a large conversion at 110°C: There was measurable conversion even at 23°C. The nickel salt shows substantially less conversion at 110°C. The zinc salt showed only small conversion at 110°C, but considerably more at 147°C. The potassium and sodium salts showed only traces of conversion even

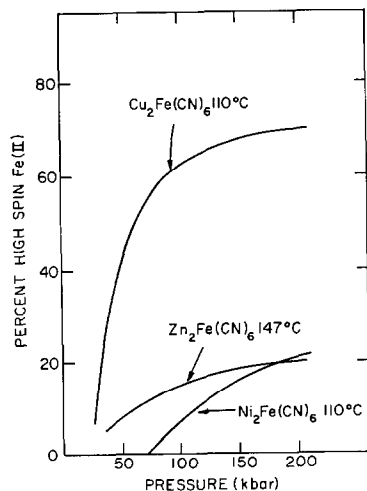


FIG. 5. Percent high-spin Fe(II) versus pressure—ferrocyanides.

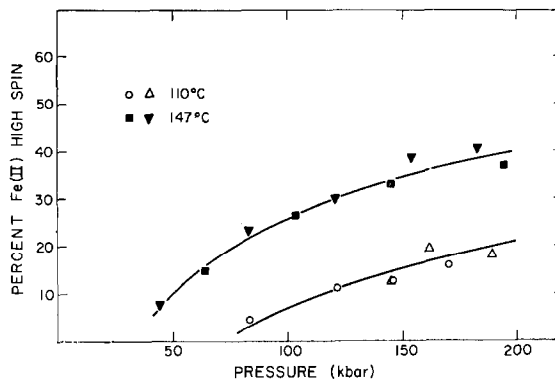


FIG. 6. Percent high-spin Fe(II) versus pressure—100 and 147°C—Ni₂Fe(CN)₆.

at 150°C and high pressure. Thus, the cation is important. Figure 6 for Ni₂Fe(CN)₆, shows that the low- to high-spin conversion increases measurably with increasing temperature.

A qualitative explanation of the phenomenon is possible. The observations on the reduction of iron with pressure indicate that the 3*d* orbitals lower in energy vis-à-vis the ligand orbitals as the pressure increases, so that iron increases its affinity for electrons. This change in energy level increases the energy difference between *t*_{2*g*} metal levels and the π* ligand orbitals, and thus reduces the degree of back donation, which weakens the metal to CN⁻ bond.

If the back donation does decrease with increasing pressure, it should be reflected in the relative change in isomer shift with pressure for the low-spin ion. As Fig. 7 reveals, this is indeed so. The potassium and sodium salts, which undergo minimum conversion, show the usual decrease in isomer shift (increase in electron density at the nucleus) due to

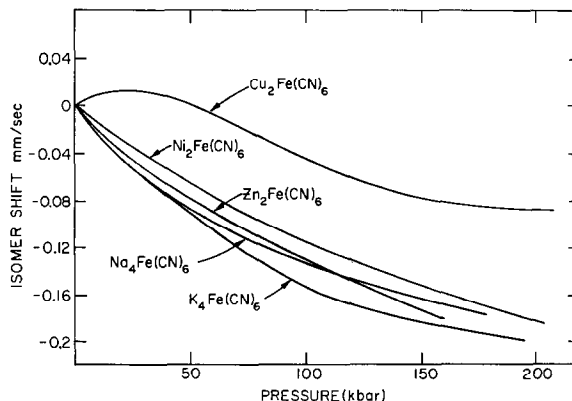


FIG. 7. Isomer shift—(relative to 1 atm) versus pressure—ferrocyanides.

changes in the sigma orbitals. The zinc salt shows a little smaller decrease, the nickel salt appreciably less, while the copper salt, which showed the maximum conversion, exhibits an actual *increase* in isomer shift with pressure in the low-pressure region. Evidently the relocalization of t_{2g} electrons due to reduced back donation, more than overcomes the usual spreading of the sigma orbitals.

The effect of the cation on the conversion is of interest. There is a difference in crystal structure between the alkali ferrocyanides and the heavy metal ferrocyanides which may be a factor. The order of the electronegativities as determined from the electrode potentials is $K^+ > Na^+ > Zn^{++} > Ni^{++} > Cu^{++}$. This is the inverse order of the conversion. Evidently the copper, which forms the most covalent bond with the nitrogen end of the ferrocyanide, perturbs the electron distribution on the cyanide most strongly in a fashion to reduce iron-to-carbon back donation. On the other hand, the potassium, which forms a strongly ionic bond with the molecular ion, offers the least perturbation.

It is of interest to investigate the effect of strain and distortion on the low- to high-spin conversion. A strained ferrocyanide site is produced by the pressure-induced reduction of ferricyanides. All of the ferricyanides reduce easily with increasing pressure, so that by 40–50 kbar at 23°C, they are 80–90% converted to the ferrocyanide. In Fig. 8, one observes the spin state as a function of pressure for the five ferrocyanides so produced. The order of the cations is essentially preserved, but in each case there is more low- to high-spin conversion at a given pressure than one observes for the corresponding ordinary ferrocyanide. Even the potassium, sodium, and zinc salts show significant conversion at 110°C.

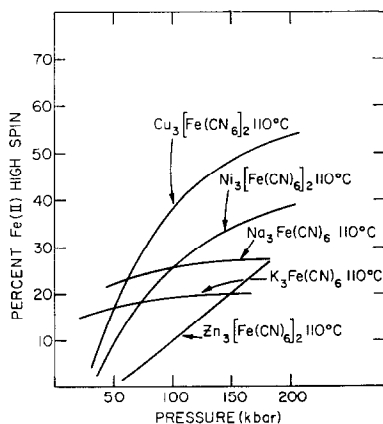


FIG. 8. Percent high-spin Fe(II) versus pressure—ferrocyanides made from ferricyanides.

The difference between these compounds and ordinary ferrocyanides is that here one has a hole either circulating among the six cyanide ions, or isolated on one of them to form a free radical. Evidently the back donation is significantly weakened by the presence of the hole.

A distortion in local symmetry at the iron site is produced by substituting for one of the cyanide ligands. The most widely studied systems are the nitroprussides, where an NO replaces the CN^- ion. The arrangement consists nominally of a low-spin ferrous ion surrounded by five CN^- ions and an NO^+ , although the actual electron distribution must be more complex (12). The Fe–NO bond length is only 1.63 Å compared with the Fe–CN distance of 1.91 Å. This strong distortion accounts for the high quadrupole splitting shown in Table I. The nitroprusside ion exhibits a very strong ligand field and even larger delocalization of the $t_{2g}(\pi)$ orbitals than does ferrocyanide. Other substitutions for a CN^- are possible. The substitution of NH_3 results in considerably less distortion, less quadrupole splitting, and a smaller degree of back donation.

Figure 9 shows the low- to high-spin conversion for a series of nitroprussides, as well as for the NH_3 substituted cyanide (13). The nitroprussides exhibit a very high degree of spin conversion, the NH_3 substituted complex shows markedly less. Evidently the distortion introduced by the substituent has an important effect on the change of bonding with pressure. Figure 10 shows the change of isomer shift with pressure for the low-spin ferrous ion. Again, those complexes which exhibit most high spin

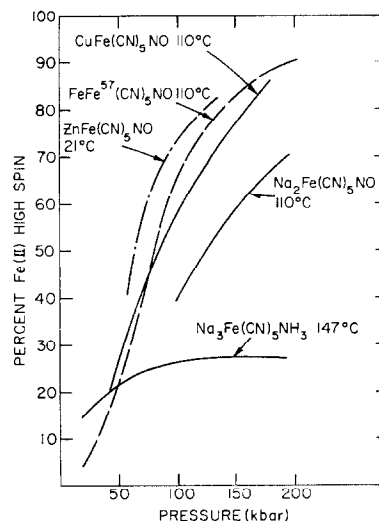


FIG. 9. Percent high-spin Fe(II) versus pressure—substituted cyanides.

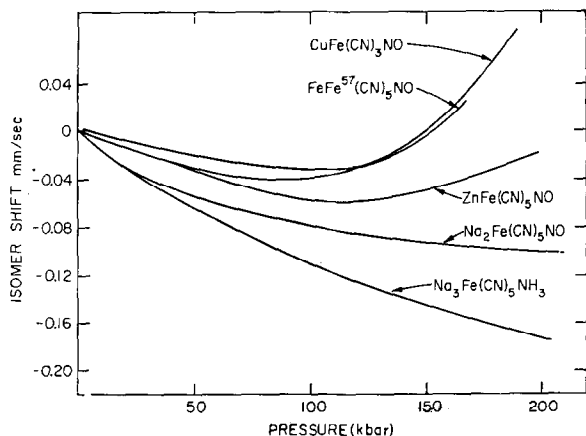


FIG. 10. Isomer shift (relative to 1 atm) versus pressure—substituted cyanides.

conversion show an actual decrease in electron density at the iron nucleus with pressure, while the NH_3 substituted complex exhibits less conversion and the usual increase in electron density with pressure.

In addition to these general studies, two compounds merit special discussion. These are Prussian blue, $\text{Fe}_4[\text{Fe}(\text{CN})_6]_3$, and ferrous nitroprusside $\text{Fe}[\text{Fe}(\text{CN})_5\text{NO}]$. In each case, we find iron in two different oxidation and/or spin states. It is possible to tag each type of site separately with ^{57}Fe and look at its behavior. We have done this with both these compounds.

Prussian blue is ferric ferrocyanide. It consists of a low-spin $\text{Fe}(\text{II})$ ion coordinated to six cyanides through the carbon, and a high-spin $\text{Fe}(\text{III})$ ion coordinated to the nitrogen (14). From Fig. 11 one observes that the high-spin $\text{Fe}(\text{III})$ transforms to high-spin $\text{Fe}(\text{II})$ very strongly with increasing pressure. As we shall see in a moment, the disappearance of $\text{Fe}(\text{III})$ high spin involves both the direct reduction and a second process. The fact that

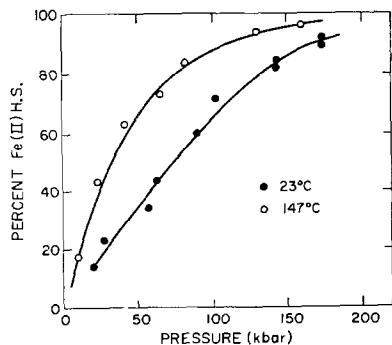


FIG. 11. Yield of high-spin $\text{Fe}(\text{II})$ from $^{57}\text{Fe}_4[\text{Fe}(\text{CN})_6]_3$.

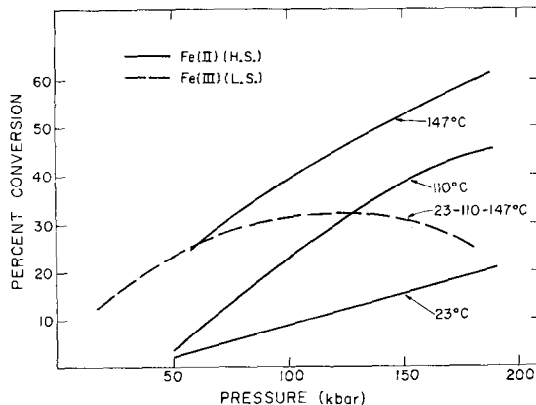
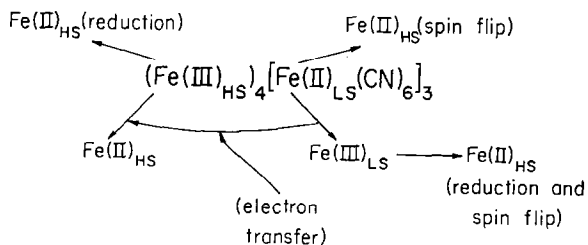


FIG. 12. Conversion versus pressure— $\text{Fe}_4[^{57}\text{Fe}(\text{CN})_6]_3$.

no low-spin iron appears in this spectrum eliminates the possibility that the change of spin state is due to isomerization of the CN^- ion. The data on $^{57}\text{Fe}[\text{Fe}(\text{CN})_5\text{NO}]$ confirm this conclusion.

In the spectra of $\text{Fe}_4[\text{Fe}^{57}(\text{CN})_6]_3$ two features appear. At moderate pressures, low-spin $\text{Fe}(\text{III})$ appears. This indicates the transfer of an electron from the low-spin $\text{Fe}(\text{II})$ of the ferrocyanide to the high-spin $\text{Fe}(\text{III})$ cation. At higher pressures the low- to high-spin transformation of the $\text{Fe}(\text{II})$ dominates. As can be seen from Fig. 12, the electron distribution between iron sites is independent of temperature, but the spin flip is not. It is of interest that the energies of the t_{2g} levels on the cation coordinated to the nitrogen lower with increasing pressure with respect to those on the iron coordinated to the carbon. At 1 atm in the ground state, the electron is on the ferrocyanide ion. From Figs. 11 and 12, one can see that at 150°C and 160 kbar, over 90% of the ferric ions present are low-spin ions (coordinated to the carbon); that is, there is over 90% probability that the electron has transferred to the cation. The processes that occur under pressure are illustrated by the following diagram.



In this diagram *reduction* refers always to ligand to metal electron transfer.

In $\text{Fe}[\text{Fe}(\text{CN})_5\text{NO}]$ the cation is a high-spin ferrous ion. With pressure, one observes for

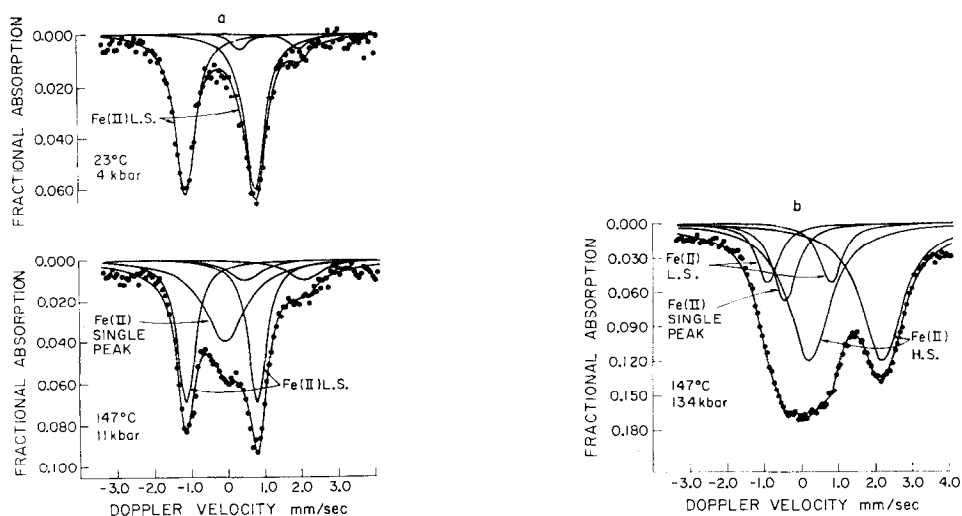


FIG. 13. (a) Spectra of $\text{Fe}^{[57}\text{Fe}(\text{CN})_5\text{NO}]$. (b) Spectra of $\text{Fe}^{[57}\text{Fe}(\text{CN})_5\text{NO}]$ continued.

$^{57}\text{Fe}[\text{Fe}(\text{CN})_5\text{NO}]$ only a moderate decrease in isomer shift and increase of quadrupole splitting typical for ionic ferrous ions. This is further evidence that the change of spin state of ferrocyanides is not due to isomerization.

As indicated earlier, the low-spin ferrous ion coordinated to the carbon of the cyanide and to the nitrogen of the NO, exhibits a very low-isomer shift, indicating that the delocalization of the 3d electrons to the NO is even stronger than that to the cyanides. There is a large quadrupole splitting because of the distortion from octahedral symmetry. As the spectra in Fig. 13a and b show, the $[\text{Fe}(\text{CN})_5\text{NO}]^{2-}$ ion exhibits two phenomena as a function of pressure. At modest pressure and high temperature, a single peak appears with essentially the same isomer shift as the quadrupole split low-spin pair. It grows with

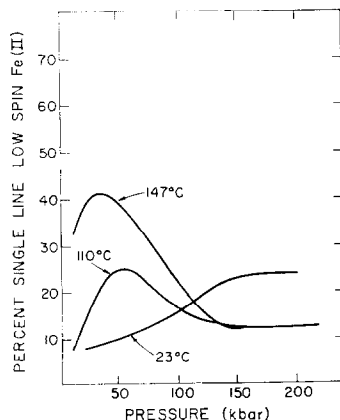


FIG. 14. Percent single line low spin Fe(II) versus pressure— $\text{Fe}^{[57}\text{Fe}(\text{CN})_5\text{NO}]$.

pressure at first, then decreases in intensity along with the original pair as the conversion to high spin Fe(II) begins to dominate. Figure 14 exhibits the amount of the single peak low-spin material as a function of temperature and pressure for $\text{Fe}^{[57}\text{Fe}(\text{CN})_5\text{NO}]$. Figure 15 shows the conversion to high spin Fe(II) for the same compound. We were able to quench in partially converted samples and obtain ir spectra on them. In Fig. 16 are represented three spectra in the region of the CN^- and NO stretching vibrations; one at atmospheric pressure, one from 35 kbar and 147°C, where there is a maximum amount of the single low-spin peak, and one from 160 kbar and 110°C where the main conversion is to high-spin Fe(II) . At one atmosphere, both peaks are at lower energy than that of the corresponding free ion, as the intraionic bonding is weakened by the strong bond to the metal. At 147°C and 35 kbar, a peak grows on the high energy

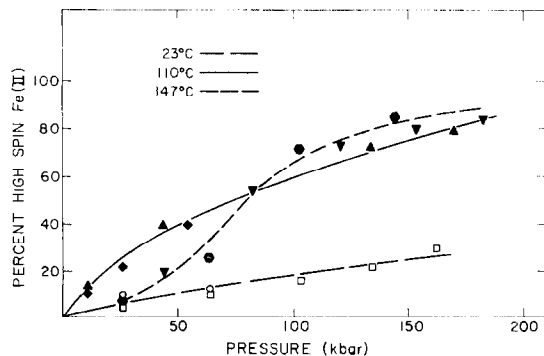


FIG. 15. Percent high-spin Fe(II) versus pressure— $\text{Fe}^{[57}\text{Fe}(\text{CN})_5\text{NO}]$.

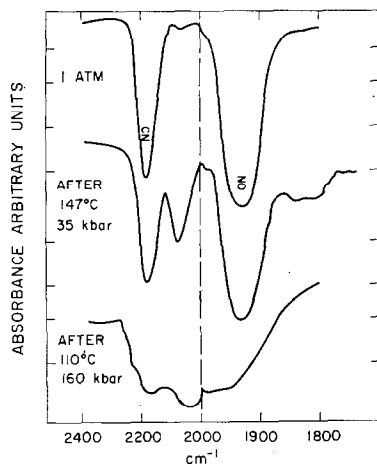


FIG. 16. IR Spectrum of $\text{Fe}[\text{Fe}(\text{CN})_5\text{NO}]$.

side of the NO stretch, near the free ion value. This corresponds to those sites where the metal to NO bond is weakened, giving a more symmetric spectrum and a single Mössbauer peak. At high pressure, the new NO stretching peak is very strong, and a shoulder appears on the high energy side of the CN stretching peak. This situation corresponds to reduced metal to ligand bonding, giving rise to the high spin $\text{Fe}(\text{II})$.

In summary, with increasing pressure, there is a relative lowering of the energy of the iron $3d$ orbitals vis-à-vis the ligand orbitals. This has important effects on both the oxidation state and

spin state of iron. An understanding of this behavior has significant consequences in the chemistry and physics of iron, and possibly also for understanding its biological activity and geophysical behavior.

References

1. H. G. DRICKAMER, in "Solids Under Pressure," pp. 357-385 (W. Paul and D. Warschauer, Eds.), McGraw-Hill Book Co., New York, 1963; H. G. DRICKAMER, *Solid State Phys.* **17**, 1-135 (1965). These reviews contain references to the original papers.
2. A. R. CHAMPION, R. W. VAUGHAN, AND H. G. DRICKAMER, *J. Chem. Phys.* **47**, 2583 (1967).
3. G. K. LEWIS, JR. AND H. G. DRICKAMER, *Proc. Natl. Acad. Sci.* **61**, 414 (1968).
4. S. C. FUNG, G. K. LEWIS, JR., AND H. G. DRICKAMER, *Proc. Natl. Acad. Sci.* **61**, 812 (1968).
5. D. C. GRENOBLE AND H. G. DRICKAMER, *Proc. Natl. Acad. Sci.* **61**, 1177 (1968).
6. S. FUNG AND H. G. DRICKAMER, *Proc. Natl. Acad. Sci.* **62**, 38 (1969).
7. W. HOLZAPFEL AND H. G. DRICKAMER, *J. Chem. Phys.* **50**, 1480 (1969).
8. H. G. DRICKAMER, G. K. LEWIS, JR., AND S. C. FUNG, *Science* **163**, 885 (1969).
9. V. N. PANYUSHKIN, G. DE PASQUALI, AND H. G. DRICKAMER, *J. Chem. Phys.* **51**, 3305 (1969).
10. D. C. FISHER, unpublished results.
11. S. C. FUNG AND H. G. DRICKAMER, *J. Chem. Phys.* **51**, 4353 (1969).
12. P. T. MANORAHAN AND H. B. GRAY, *J. Amer. Chem. Soc.* **87**, 3340 (1965).
13. S. C. FUNG AND H. G. DRICKAMER, *J. Chem. Phys.* **51**, 4360 (1969).
14. M. B. ROBIN, *Inorg. Chem.* **1**, 337 (1962).